Acta Pharmacologica Sinica (2017) 38: 146–155
 1671-4083/17
www.nature.com/aps

Original Article

Discovery, synthesis, biological evaluation and structure-based optimization of novel piperidine derivatives as acetylcholine-binding protein ligands

Jian SHEN[#], Xi-cheng YANG[#], Ming-cheng YU, Li XIAO, Xun-jie ZHANG, Hui-jiao SUN, Hao CHEN, Guan-xin PAN, Yu-rong YAN, Si-chen WANG, Wei LI[*], Lu ZHOU[*], Qiong XIE, Lin-qian YU, Yong-hui WANG, Li-ming SHAO[*]

Department of Medicinal Chemistry, School of Pharmacy, Fudan University, Shanghai 201203, China

Abstract

The homomeric α7 nicotinic receptor (α7 nAChR) is widely expressed in the human brain that could be activated to suppress neuroinflammation, oxidative stress and neuropathic pain. Consequently, a number of α7 nAChR agonists have entered clinical trials as anti-Alzheimer's or anti-psychotic therapies. However, high-resolution crystal structure of the full-length α7 receptor is thus far unavailable. Since acetylcholine-binding protein (AChBP) from *Lymnaea stagnalis* is most closely related to the α-subunit of nAChRs, it has been used as a template for the N-terminal domain of α-subunit of nAChR to study the molecular recognition process of nAChR-ligand interactions, and to identify ligands with potential nAChR-like activities. Here we report the discovery and optimization of novel acetylcholine-binding protein ligands through screening, structure-activity relationships and structure-based design. We manually screened in-house CNS-biased compound library *in vitro* and identified compound **1**, a piperidine derivative, as an initial hit with moderate binding affinity against AChBP (17.2% inhibition at 100 nmol/L). During the 1st round of optimization, with compound **2** (21.5% inhibition at 100 nmol/L) as the starting point, 13 piperidine derivatives with different aryl substitutions were synthesized and assayed *in vitro*. No apparent correlation was demonstrated between the binding affinities and the steric or electrostatic effects of aryl substitutions for most compounds, but compound **14** showed a higher affinity (K_i=105.6 nmol/L) than nicotine (K_i=777 nmol/L). During the 2nd round of optimization, we performed molecular modeling of the putative complex of compound **14** with AChBP, and compared it with the epibatidine-AChBP complex. The results suggested that a different piperidinyl substitution might confer a better fit for epibatidine as the reference compound. Thus, compound **15** was designed and identified as a highly affinitive acetylcholine-binding protein ligand. In this study, through two rounds of optimization, compound **15** (K_i=2.8 nmol/L) has been identified as a novel, piperidine-based acetylcholine-binding protein ligand with a high affinity.

Keywords: α7 nAChR; acetylcholine-binding protein ligands; piperidine derivatives; molecular modeling; psychotic disorders

Acta Pharmacologica Sinica (2017) 38: 146–155; doi: 10.1038/aps.2016.124; published online 5 Dec 2016

Introduction

Acetylcholine is an important neurotransmitter in the central nervous system (CNS). Dysfunctional acetylcholine signaling is associatedwith significant pathological conditions (*eg*, Alzheimer's disease[1], Parkinson's disease[2–5] and schizophrenia[6–8]). Its cholinergic effects are mediated through either muscarinic (mAChR) or nicotinic (nAChR) receptors. Cumulative evidence suggests that the homomeric α_7 receptor, one subtype of the most widely expressed nicotinic receptor in the human brain, could be activated to suppress neuroinflammation[9, 10], oxidative stress[9, 11] and neuropathic pain[12] in animal models. Moreover, improvement in the triad of positive symptoms, negative symptoms and cognitive dysfunction in schizophrenia is shown to be mediated by the α_7 receptor in both preclinical and clinical studies[13–15]. Several α_7 nAChR agonists (*eg,* tropisetron[16, 17], GTS-21[18, 19], TC-5619 (bradanicline)[20–22], EVP-6124[23], ABT-126[24], AQW051[25], Figure 1) have entered clinical trials as anti-Alzheimer's or anti-psychotic therapies. FORUM Pharmaceuticals Inc recently completed a phase-III clinical trial of EVP-6124 as an adjunctive pro-cognitive treatment in schizophrenia subjects during chronic, stable, atypical antipsychotic therapy (ClinicalTrials.gov Identifier: NCT01716975). Additional α_7 nAChR agonists are expected to move into clinical trials to address the unmet medical needs

[#] These authors contributed equally to this work.
[*]To whom correspondence should be addressed.
E-mail limingshao@fudan.edu.cn (Li-ming SHAO);
wei-li@fudan.edu.cn (Wei LI);
zhoulu@fudan.edu.cn (Lu ZHOU)
Received 2016-07-21 Accepted 2016-09-20

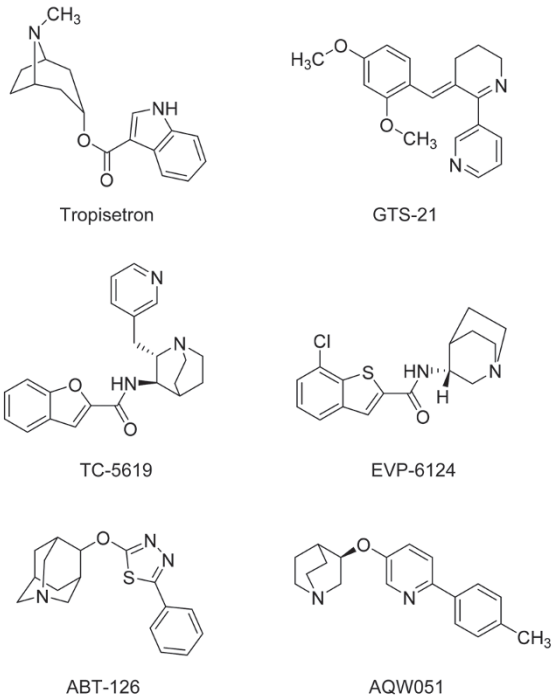

Figure 1. Structural formulae of α7 nAChR agonists under clinical development.

of patients suffering from psychotic disorders. Unfortunately, similar to other ligand-gated ion channels (LGICs) such as 5-HT_3 and $GABA_A$, there is no available high-resolution crystal structure of the α_7 receptor. However, some evidence-based hypotheses[26–28] and theoretical models[29–31] have been developed.

Acetylcholine-binding protein (AChBP) is a soluble protein separated from *Lymnaea stagnalis*[32], which is most closely related to the α-subunit of nAChRs. Nearly all residues conserved within the nAChR family are present in AChBP, including those relevant to ligand binding. AChBP also binds to known nAChR agonists and competitive antagonists, such as acetylcholine, nicotine, d-tubocurarine and α-bungarotoxin[33]. Therefore, AChBP could be utilized as a template for the N-terminal domain of an α-subunit of nAChR to study the molecular recognition process of nAChR-ligand interactions[34–37] and to identify ligands with potential nAChR-like activities[38–40].

Based on the previously described AChBP-based binding assay[41], our in-house CNS-biased compound library was manually screened and compound **1**, a piperidine derivative, was identified as an initial hit with moderate binding affinity against AChBP (17.2% inhibition at 100 nmol/L). Since the pyridine substructure is considered to be a privileged substructure for typical nAChR agonists (such as nicotine and epibatidine) and methoxypyridineis also common in nAChR ligands[42–44], the naphthalene substructure of compound **1** was changed to a pyridine ring in compound **2**, which marginally increased binding to AChBP (21.5% inhibition at 100 nmol/L). Moreover, with compound **2** as the starting point of this study, we conducted structure-activity relationship (SAR) analysis, and structure-based optimization, which eventually yielded a low-nanomolar affinity compound (compound **15**) against AChBP, as shown in Scheme 1.

Materials and methods

Chemistry

Chemicals were purchased from Sigma Aldrich (Sigma-Aldrich Shanghai Trading Co Ltd, Shanghai, China),

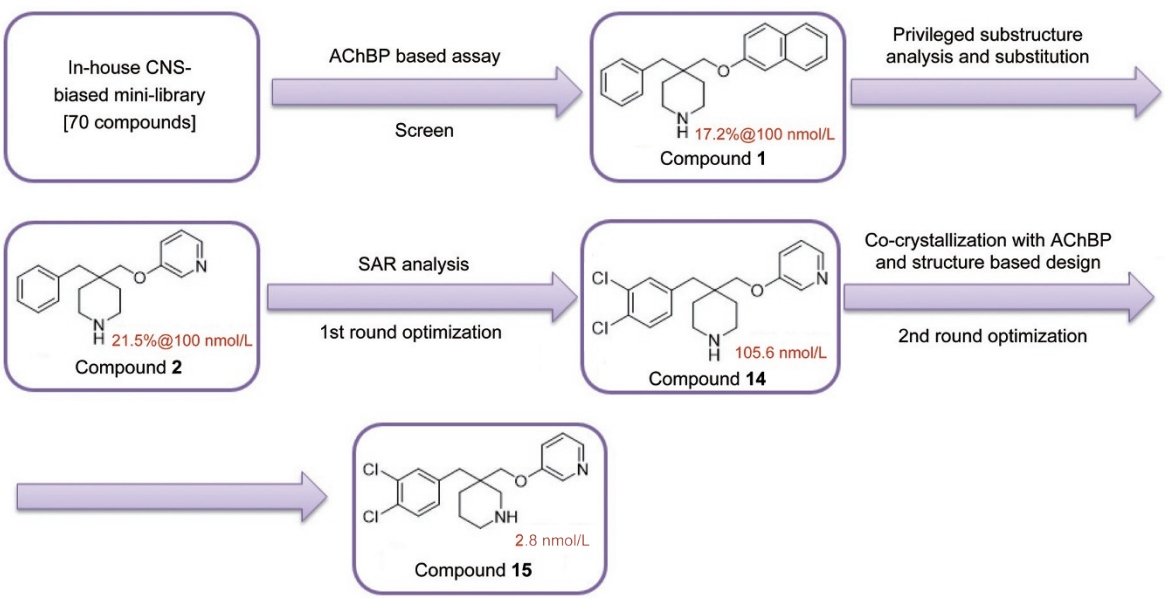

Scheme 1. The discovery path of compound **15** as a potent AChBP ligand.

AcrosOrganics (Fisher Scientific Worldwide (Shanghai) Co, Ltd, Shanghai, China), Energy Chemical (Sun Chemical Technology (Shanghai) Co, Ltd, Shanghai, China) and Shanghai Chemical Reagent Company (Shanghai, China) and were used directly without further purification. All compounds were purified by silica gel thin-layer chromatography (>95%), and their structures were determined with nuclear magnetic resonance spectra and low-resolution mass spectra. ^{1}H spectra were recorded in DMSO-d^6 or $CDCl_3$ on Varian Mercury-300 or Varian Mercury-400 instruments. Mass spectra were generated with electric ionization (ESI) produced by an HP5973N analytical mass spectrometer.

General procedure for the preparation of 2a and 15a

A solution of commercially available substituted piperidine derivative (12.7 mmol) in anhydrous DCM (100 mL) was cooled to 0 °C. Tert-butyldicarbonate (2.6 g, 12.1 mmol) in DCM (20 mL) was added drop-wise into solution. After being stirred for 10 min, the reaction mixture was allowed to adjust to room temperature and stirred overnight. After dilution with water, the crude product was extracted with DCM (100 mL×2). The combined organic extracts were washed with hydrochloric acid (0.5 mol/L, 50 mL), and brine (100 mL), dried over Na_2SO_4, filtered, and concentrated to yield compounds **2a** and **15a**. The crude product was used without further purification.

Detailed analytical information can be found in the supporting information.

General procedure for the preparation of 2b–15b

A solution of commercially available lithium diisopropylamide (2 mol/L, 21.7 mmol) in anhydrous THF (100 mL) was cooled to -78 °C. Compound **2a** (12.1 mmol) in anhydrous THF (20 mL) was added drop-wise into the solution. After being stirred for 10 min, the reaction mixture was allowed to adjust to -30 °C and stirred for 30 min. Various substituted benzyl bromides (24.2 mmol) in anhydrous THF (20 mL) were added drop-wise into the solution, which was cooled to -78 °C again. After being stirred for 2 h at -78 °C, the solution was adjusted to room temperature and stirred overnight. The reaction mixture was quenched by the addition of saturated ammonium chloride solution (30 mL) at 0 °C. After dilution with water, the crude product was extracted with ethyl acetate (200 mL×2). Combined organic extracts were washed with water (100 mL) and brine (100 mL), dried over Na_2SO_4, filtered, and concentrated. The crude product was purified by column chromatography over silica using petroleum ether/ethyl acetate (15/1) to yield compounds **2b–15b**.

Detailed analytical information can be found in the supporting information.

General procedure for the preparation of 2c–15c

A solution of compounds **2b–15b** (1.39 mmol) in anhydrous THF (50 mL) was cooled to 0 °C. Lithium aluminum hydride (1 mol/L, 1.39 mmol) in anhydrous THF was added drop-wise into the solution. After being stirred at 0 °C for 1 h, the reaction mixture was quenched by the addition of saturated ammonium chloride solution (10 mL) at 0 °C. After dilution with water, the crude product was extracted with ethyl acetate (100 mL×2). The combined organic extracts were washed with water (100 mL) and brine (100 mL), dried over Na_2SO_4, filtered, and concentrated to yield compounds **2c–15c**. The crude product was used without further purification.

Detailed analytical information can be found in the supporting information.

General procedure for the preparation of 2d–15d

A solution of compounds **2c–15c** (0.69 mmol) in anhydrous DMF (8 mL) was cooled to 0 °C. Sodium hydroxide (3.45 mmol) was added to the solution and stirred for 15 min at room temperature. Then, 3-fluoropyridine (3.45 mmol) was added and the reaction mixture was heated to 75 °C for 10 h. The reaction mixture was quenched by the addition of saturated ammonium chloride solution (30 mL) at 0 °C. After dilution with water, the crude product was extracted with ethyl acetate (30 mL×2). The combined organic extracts were washed with water (10 mL) and brine (10 mL), dried over Na_2SO_4, filtered, and concentrated. The crude product was purified by column chromatography over silica using petroleum ether/ethyl acetate (5/1) to yield compounds **2d–15d**.

Detailed analytical information can be found in the supporting information.

General procedure for the preparation of 2–15

Compounds **2d–15d** (0.24 mmol) were dissolved in DCM (3 mL) along with TFA (1 mL), and the reaction mixture was stirred at room temperature for 1 h and then concentrated. The crude product was dissolved in DCM (50 mL) and basified with sodium hydroxide solution (20%, 2 mL). Organic extracts were dried over Na_2SO_4, filtered, and concentrated. The crude product was purified by column chromatography over silica using DCM/methanol (10/1) to yield compounds **2–15**.

3-[(4-benzylpiperidin-4-yl)methoxy]pyridine (2)

Pale yellow oil 99%. ^{1}H NMR (400 MHz, $CDCl_3$) δ 9.80–9.00 (brs, 1H), 8.33–8.30 (brs, 1H), 8.22–8.19 (brs, 1H), 7.24–7.14 (m, 5H), 7.02–6.98 (m, 2H), 3.67 (s, 2H), 3.40–3.20 (m, 4H), 2.86 (s, 2H), 1.94–1.88 (m, 4H). ESI-MS (*m/z*): 283 $[M+H]^+$. HRMS (*m/z*): calculated for $C_{18}H_{22}N_2O$ $[M+H]^+$, 283.1810; observed, 283.1812.

3-{[4-(2-chlorobenzyl)piperidin-4-yl]methoxy}pyridine (3)

Pale yellow oil 99%. ^{1}H NMR (400 MHz, $CDCl_3$) δ 8.23–8.21 (m, 1H), 8.20–8.16 (m, 1H), 7.28–7.17 (m, 1H), 7.16–7.06 (m, 5H), 3.80 (s, 2H), 3.00–2.90 (m, 2H), 2.84–2.80 (m, 2H), 2.35–2.25 (brs, 1H), 1.78–1.59 (m, 4H). ESI-MS (*m/z*): 317 $[M+H]^+$. HRMS (*m/z*): calculated for $C_{18}H_{21}ClN_2O$ $[M+H]^+$, 317.1421; observed, 317.1415.

3-{[4-[2-(trifluoromethyl)benzyl]piperidin-4-yl}methoxy}pyridine (4)

Pale yellow oil 99%. ^{1}H NMR (400 MHz, $CDCl_3$) δ 8.30–8.19

(s, 2H), 7.68–7.62 (m, 1H), 7.48–7.41 (m, 1H), 7.40–7.35 (m, 1H), 7.35–7.25 (m, 1H), 7.18–7.10 (m, 1H), 3.98–3.92 (m, 2H), 3.38–3.34 (m, 2H), 3.12–3.09 (m, 2H), 2.01–2.00 (m, 4H). ESI-MS (*m/z*): 351 $[M+H]^+$. HRMS (*m/z*): calculated for $C_{19}H_{21}F_3N_2O$ $[M+H]^+$, 351.1684; observed, 351.1669.

3-{[4-(2-methylbenzyl)piperidin-4-yl]methoxy}pyridine (5)

Pale yellow oil 98%. ^{1}H NMR (400 MHz, CD_3OD) δ 8.29–8.28 (m, 1H), 8.19–8.17 (m, 1H), 7.50–7.46 (m, 1H), 7.43–7.39 (m, 1H), 7.18–7.08 (m, 4H), 3.98 (s, 2H), 3.28–3.14 (m, 4H), 2.97 (s, 2H), 2.32 (s, 3H), 2.01–1.94 (m, 2H), 1.92–1.82 (m, 2H). ESI-MS (*m/z*): 297 $[M+H]^+$. HRMS (*m/z*): calculated for $C_{19}H_{24}N_2O$ $[M+H]^+$, 297.1967; observed, 297.1962.

3-{[4-(3-chlorobenzyl)piperidin-4-yl]methoxy}pyridine (6)

Pale yellow oil 99%. ^{1}H NMR (400 MHz, $CDCl_3$) δ 8.36–8.25 (m, 1H), 7.95–7.75 (m, 2H), 7.07–6.97 (m, 2H), 6.92-6.79 (m, 2H), 3.90–3.75 (m, 2H), 3.40–3.20 (m, 5H), 2.84–2.65 (m, 2H), 1.95–1.65 (m, 4H). ESI-MS (*m/z*): 317 $[M+H]^+$. HRMS (*m/z*): calculated for $C_{18}H_{21}ClN_2O$ $[M+H]^+$, 317.1421; observed, 317.1417.

3-{{4-[3-(trifluoromethyl)benzyl]piperidin-4-yl}methoxy}pyridine (7)

Pale yellow oil 95%. ^{1}H NMR (600 MHz, $CDCl_3$) δ 8.35–8.33 (m, 1H), 8.26–8.24 (m, 1H), 7.47–7.43 (m, 1H), 7.35-7.31 (m, 2H), 7.27–7.22 (m, 2H), 7.20–7.16 (m, 1H), 4.91–4.88 (brs, 1H), 3.68 (s, 2H), 3.18–3.12 (m, 2H), 3.05–3.00 (m, 2H), 2.96 (s, 2H), 1.78–1.73 (m, 4H). ESI-MS (*m/z*): 351 $[M+H]^+$. HRMS (*m/z*): calculated for $C_{19}H_{21}F_3N_2O$ $[M+H]^+$, 351.1684; observed, 351.1674.

3-{[4-(3-methylbenzyl)piperidin-4-yl]methoxy}pyridine (8)

Pale yellow oil 99%. ^{1}H NMR (600 MHz, $CDCl_3$) δ 8.36–8.35 (m, 1H), 8.24–8.22 (m, 1H), 7.25–7.19 (m, 2H), 7.12–7.09 (m, 1H), 7.01–6.99 (m, 1H), 6.87–6.85 (m, 2H), 4.46–4.45 (brs, 1H), 3.70 (s, 2H), 3.16–3.11 (m, 2H), 3.06–3.01 (m, 2H), 2.85 (s, 2H), 2.21 (s, 3H), 1.76–1.72 (m, 4H). ESI-MS (*m/z*): 297 $[M+H]^+$. HRMS (*m/z*): calculated for $C_{19}H_{24}N_2O$ $[M+H]^+$, 297.1967; observed, 297.1957.

3-{[4-(4-chlorobenzyl)piperidin-4-yl]methoxy}pyridine (9)

Pale yellow oil 95%. ^{1}H NMR (600 MHz, CD_3OD) δ 8.72–8.21 (m, 1H), 8.11–8.05 (m, 1H), 7.10–7.08 (m, 1H), 7.06–6.81 (m, 5H), 3.52 (s, 2H), 3.31–3.25 (m, 2H), 3.21–3.12 (m, 2H), 2.70 (s, 2H), 1.91–1.78 (m, 4H). ESI-MS (*m/z*): 317 $[M+H]^+$. HRMS (*m/z*): calculated for $C_{18}H_{21}ClN_2O$ $[M+H]^+$, 317.1421; observed, 317.1407.

3-{{4-[4-(trifluoromethyl)benzyl]piperidin-4-yl}methoxy}pyridine (10)

Pale yellow oil 95%. ^{1}H NMR (400 MHz, CD_3OD) δ 8.32–8.31 (m, 1H), 8.20–8.18 (m, 1H), 7.56–7.53 (m, 2H), 7.51–7.47 (m, 1H), 7.43–7.39 (m, 1H), 7.37–7.34 (m, 2H), 3.86 (s, 2H), 3.33–3.28 (m, 2H), 3.24–3.16 (m, 2H), 3.05 (s, 2H), 1.94–1.80 (m, 4H). ESI-MS (*m/z*): 351 $[M+H]^+$. HRMS (*m/z*): calculated for $C_{19}H_{21}F_3N_2O$ $[M+H]^+$, 351.1684; observed, 351.1669.

3-{[4-(4-methylbenzyl)piperidin-4-yl]methoxy)}pyridine (11)

Pale yellow oil 96%. ^{1}H NMR (400 MHz, CD_3OD) δ 8.32–8.31 (m, 1H), 8.20–8.17 (m, 1H), 7.51–7.47 (m, 1H), 7.43–7.39 (m, 1H), 7.06–7.00 (m, 4H), 3.83 (s, 2H), 3.42–3.36 (m, 2H), 3.34–3.26 (m, 2H), 2.91 (s, 2H), 2.26 (s, 3H), 1.96–1.84 (m, 4H). ESI-MS (*m/z*): 297 $[M+H]^+$. HRMS (*m/z*): calculated for $C_{19}H_{24}N_2O$ $[M+H]^+$, 297.1967; observed, 297.1966.

3-{{4-[(1,1'-biphenyl)-4-ylmethyl]piperidin-4-yl}methoxy}pyridine (12)

Pale yellow oil 99%. ^{1}H NMR (400 MHz, CD_3OD) δ 8.33–8.31 (m, 1H), 8.19–8.17 (m, 1H), 7.56–7.53 (m, 2H), 7.49–7.45 (m, 3H), 7.42–7.36 (m, 3H), 7.32–7.27 (m, 1H), 7.20–7.18 (m, 2H), 3.85 (s, 2H), 3.40–3.34 (m, 2H), 3.29–3.22 (m, 2H), 2.96 (s, 2H), 1.96–1.84 (m, 4H). ESI-MS (*m/z*): 359 $[M+H]^+$. HRMS (*m/z*): calculated for $C_{24}H_{26}N_2O$ $[M+H]^+$, 359.2123; observed, 359.2102.

3-{[4-(2,3-dichlorobenzyl)piperidin-4-yl]methoxy}pyridine (13)

Pale yellow oil 96%. ^{1}H NMR (400 MHz, CD_3OD) δ 8.20–8.15 (m, 2H), 7.43–7.37 (m, 3H), 7.24–7.15 (m, 2H), 4.00 (s, 2H), 3.15 (s, 2H), 3.11–3.04 (m, 2H), 3.02–2.95 (m, 2H), 1.88–1.75 (m, 4H). ESI-MS (*m/z*): 351 $[M+H]^+$. HRMS (*m/z*): calculated for $C_{18}H_{20}Cl_2N_2O$ $[M+H]^+$, 351.1031; observed, 351.1008.

3-{[4-(3,4-dichlorobenzyl)piperidin-4-yl]methoxy}pyridine (14)

Pale yellow oil 98%. ^{1}H NMR (400 MHz, CD_3OD) δ 8.31–8.29 (m, 1H), 8.19–8.17 (m, 1H), 7.42–7.37 (m, 3H), 7.26–7.25 (m, 1H), 7.07–7.03 (m, 1H), 3.81 (s, 2H), 3.22–3.15 (m, 2H), 3.12–3.04 (m, 2H), 2.89 (s, 2H), 1.84–1.70 (m, 4H). ESI-MS (*m/z*): 351 $[M+H]^+$. HRMS (*m/z*): calculated for $C_{18}H_{20}Cl_2N_2O$ $[M+H]^+$, 351.1031; observed, 351.1021.

3-{[3-(3,4-dichlorobenzyl)piperidin-3-yl]methoxy}pyridine (15)

Pale yellow oil 96%. ^{1}H NMR (400 MHz, $CDCl_3$) δ 8.36–8.34 (m, 1H), 8.25–8.22 (m, 1H), 7.28–7.19 (m, 4H), 6.94–6.90 (m, 1H), 3.82–3.78 (m, 1H), 3.72–3.68 (m, 1H), 2.90–2.82 (m, 3H), 2.78–2.69 (m, 3H), 2.36–2.22 (brs, 1H), 1.70–1.54 (m, 3H), 1.50–1.42 (m, 1H). ESI-MS (*m/z*): 351 $[M+H]^+$. HRMS (*m/z*): calculated for $C_{18}H_{20}Cl_2N_2O$ $[M+H]^+$, 351.1031; observed, 351.1023.

AChBP-based [^{3}H]-epibatidine binding assay

The inhibition of [^{3}H]-epibatidine binding with Ls-AChBP was conducted according to previously reported methods[41]. In brief, Ls-AChBP was diluted in PBS-Tris binding buffer (final concentration of 1.4 mmol/L KH_2PO4, 4.3 mmol/L Na_2HPO_4, 137 mmol/L NaCl, 2.7 mmol/L KCl, 20 mmol/L Trizma base, 4% DMSO, 0.05% Tween 20, pH 7.4) to obtain a quantity of 1.3 ng per well. AChBP was incubated with 10^{-4}–10^{-11} mol/L ligands in the presence of approximately 1.5 nmol/L [^{3}H]-epibatidine. Displacement of [^{3}H]-epibatidine was recorded to represent binding to AChBP. Five or six log-dilution concentrations of representative compounds were tested in duplicate. The IC_{50} (concentration of the compound that produces 50% inhibition of binding) was determined by least squares non-linear regression using GraphPad Prism software. Nicotine

served as the positive control. The results of the binding assay revealed that the affinity of nicotine was similar to a previous report (K_i=777.7 nmol/L in our article *vs* K_i=478.0 nmol/L in reported article).

Molecular modeling

All molecular models were implemented based on the molecular modeling packages in Schrodinger Maestro 10.1. The structures of epibatidine, compound **14**, **(S)-15**, and **(R)-15** were built and optimized. The crystal complex of AChBP in complex with epibatidine was acquired from the RCSB protein data bank (PDB ID: 2BYQ) and appropriately treated by the protein preparation wizard module. The Glide function, available in the packages, was employed for molecular docking. The procedures were as follows: (1) ligand preparation (the Ligprep module was used to create several conformations of the ligand), (2) receptor grid generation, and (3) ligand docking. For the receptor grid generation procedure, the residues Tyr 55, Tyr 188, Ser 189 and Tyr 195 were chosen as the 'Rotatable Groups' because the exact conformations of these residues were flexible within several reported structures.

To validate the docking methodology, epibatidine was chosen as the test ligand and the RMSD value was calculated using the core pattern comparison. The RMSD value (1.33–2.5) confirmed the reliability of the docking method. Finally, compound **14** was docked to AChBP to provide putative docked models.

The hydrogen bond, cation-π interactions, π–π interactions, as well as the measurements of the distances of certain atoms, were elucidated by the software Pymol 1.5.0.3. The 2D diagram of the putative binding mode was produced by Schrodinger Maestro 10.1.

Results

Chemistry

The piperidine derivatives were prepared in a five-step procedure as demonstrated in Scheme 2. The addition of a Boc group to a commercially available ethyl piperidine-4-carboxylate yielded compound **2a**. The Boc-protect compound **2a** reacted with various substituted benzyl bromide in the presence of LDA to afford the corresponding nucleophilic substitution products (compound **2b–14b**) in 45%–58% yields. The alcohol compounds **2c–14c** were synthesized via reduction using a $LiAlH_4$ solution at 0 °C. The reaction of compounds **2c–14c** with 3-fluoropyridine and subsequent deprotection of the Boc group by TFA furnished the target compounds **2–14**.

The synthesis of compound **15** is described in Scheme 3 utilizing a procedure similar to that used for compounds **2–14**.

Biological evaluation

The binding data of the synthesized compounds are shown in Table 1. Compared with nicotine, most of the compounds displayed slightly higher binding affinities for AChBP at a test concentration of 100 nmol/L. Compound **14** displayed a 7-fold higher binding affinity when compared to nicotine.

Molecular docking

To elucidate the binding mode of compound **14**, the molecular docking strategy was utilized using the epibatidine-bound Ls-AChBP (PDB: 2BYQ). As shown in Figure 2, compound **14** was completely buried within the protein at the interface between the principal side of the interface and the complementary side.

Each subunit consisted of an N-terminal α-helix, two short α3 helices, and a 10-stranded β-sandwich core. On the principal side, the nitrogen atom, which served as the protonation center in the piperidine ring of compound **14** at physiological pH, resided within hydrogen-bonding distance of the backbone carbonyl atom of Tyr 93. Moreover, three cation-π interactions were predicted between the protonated nitrogen atom and the phenyl groups of Tyr 188 and Tyr 195 as well as the indole group of Trp 147. The 3,4-dichloro aryl formed a T-shaped π-π interaction with Trp 147. On the complementary side, the 3,4-dichloro aryl entered into a hydrophobic subpocket formed by Ile 106, Phe 117, Ala 107, Met 116, and Val 108. Alternatively, the pyridine ring occupied another pocket

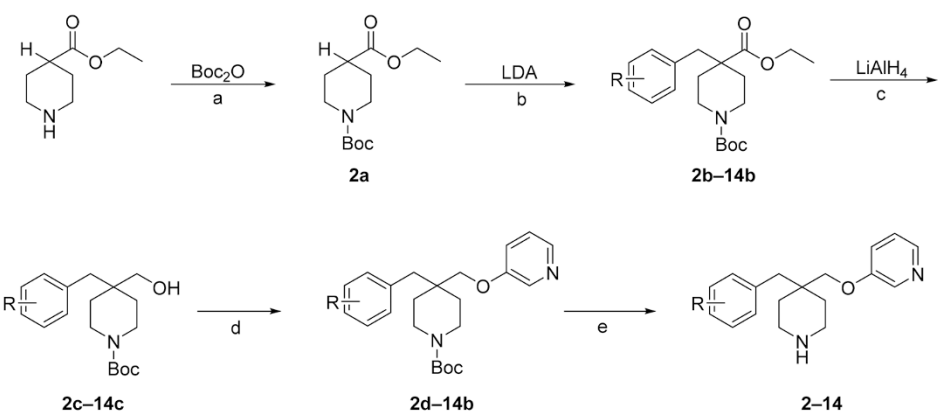

Scheme 2. Synthesis of the piperidine derivatives. Reagents and conditions: a) Boc_2O, DCM, RT, overnight (98%); b) substituted benzyl bromide, LDA, THF, -78 °C-RT, overnight (75%–86%); c) $LiAlH_4$, THF, 0 °C, 1 h (95%–98%); d) NaH, 3-Fluoropyridine, DMF, 75 °C, overnight (78%–86%); e) TFA, DCM, RT, 1 h (94%–98%).

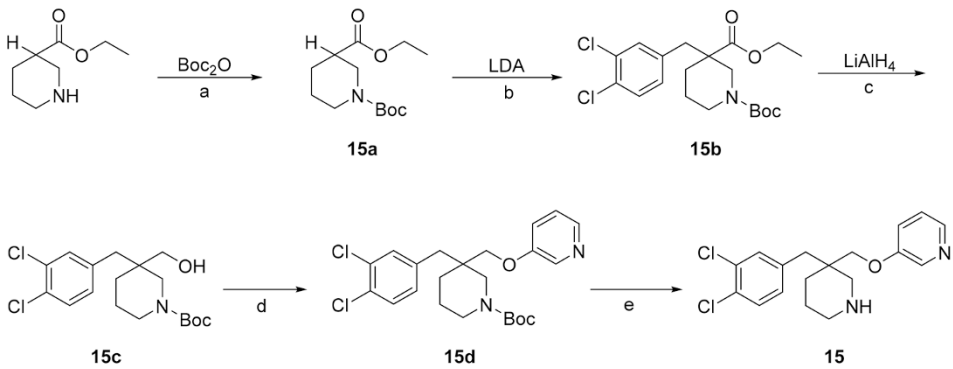

Scheme 3. Synthesis of compound **15**. Reagents and conditions: a) Boc_2O, DCM, RT, overnight (98%); b) 3,4-Dichlorobenzyl bromide, LDA, THF, -78 °C-RT, overnight (75%–86%); c) $LiAlH_4$, THF, 0 °C, 1 h (95%–98%); d) NaH, 3-Fluoropyridine, DMF, 75 °C, overnight (78%–86%); e) TFA, DCM, RT, 1 h (94%–98%).

Table 1. Binding affinities of compounds **1–15** for AChBP at 100 nmol/L.

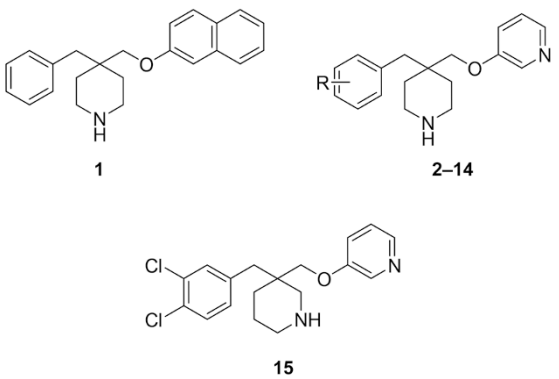

Compound	R	Binding affinity (%, inhibition at 100 nmol/L)	IC_{50} (nmol/L)
1		17.2	
2	H	21.5	
3	*o*-Cl	25.0	
4	*o*-CF_3	17.5	
5	*o*-CF_3	19.2	
6	*m*-Cl	29.6	
7	*m*-CF_3	27.4	
8	*m*-CF_3	27.4	
9	*p*-Cl	23.6	
10	*p*-CF_3	28.3	
11	*p*-CF_3	30.7	
12	*p*-Phenyl	26.5	
13	2,3-diCl	30.8	
14	3,4-diCl	47.4	105.6±0.8
15		96.9	2.8±0.2
Nicotine		21.5	777.7±8.1
Epibatidine		95.8	3.6±0.1

comprising Ser 189, Tyr 55, Cys 190, and Gln 57. The pyridine ring also shared a π–π interaction with the Cys 190-Cys 191 ring.

Discussion

With the purpose of finding novel AChBP ligands, our in-house CNS-biased compound library was screened manually *in vitro*, and compound **1**, a piperidine derivative, was chosen as the starting hit for this study. With the substructure of naphthalene changed to the privileged pyridine for compound **1**, we used compound **2** as the prototype compound for further optimization. A series of compounds with different aryl substitutions were designed and synthesized. Most compounds demonstrated somewhat higher binding affinities against AChBP than compound **2** and nicotine at 100 nmol/L. *Para*- or *meta*-substitutedaryl substitution was associated with marginal increase of affinities compared with *ortho*-substituted aryl substitution. No definite correlation between binding affinities and the steric or electrostatic effects of substituted aryl substitutions was observed. During this 1st optimization, the affinity was optimized for compound **14**, which was 7-fold higher than that of nicotine.

Molecular docking was utilized to predict the binding mode of compound **14** for further structure optimization. Epibatidine was reported to have the highest binding affinity with AChBP in natural products comprising an aromatic ring and an endocyclic secondary amino group[45]. These two groups were positioned at an optimal distance and an optimal relative spatial orientation to provide ideal interactions with the residues at the binding site[36, 46]. Minimal changes in the chemical structure of these compounds have been found to exert profound effects on their pharmacological properties[42]. As shown in Figure 3, the overlapped conformation of epibatidine versus compound **14** suggested that the protonation center located in the piperidine ring of compound **14** at physiological pH was within the hydrogen-bonding distance of the back-

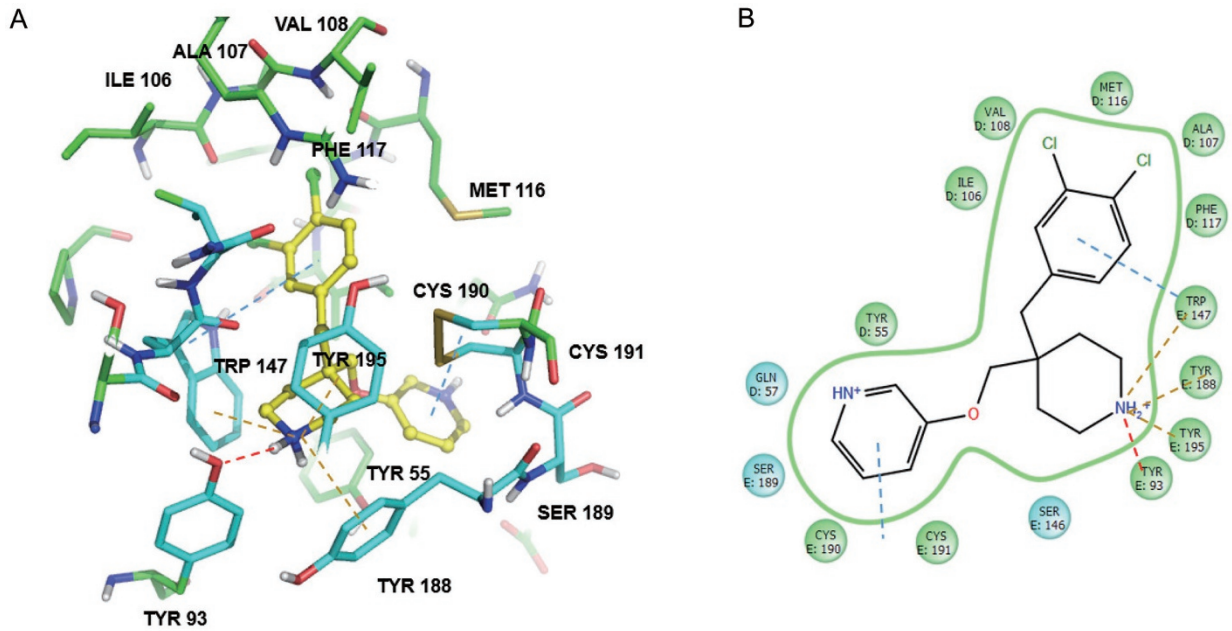

Figure 2. A putative binding mode of compound **14** in complex with Ls-AChBP. The hydrogen-bond (red dash), the cation-π interactions (brown dash) and the π–π interactions (blue dash) were shown. (A) The 3D view of the putative binding mode of compound **14** (colored by yellow). The principal side chain (colored by blue) and the complementary side (colored by green) were shown. (B) The 2D view of the putative binding mode of compound **14**.

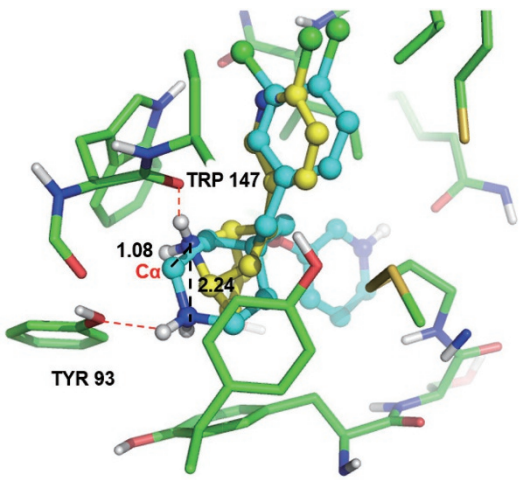

Figure 3. Comparison of the binding mode of compound **14** (colored by blue) with that of epibatidine (colored by yellow). The hydrogen bonds (red dash) as well as the distance (black dash) between the alpha-carbon (Cα) and the nitrogen atom in aliphatic ring of compound **14** with the nitrogen atom in aliphatic ring of epibatidine were shown.

bone carbonyl atom of Tyr 93. In contrast, epibatidine formed a hydrogen-bond between the potentially protonated nitrogen atom of the aliphatic ring and the backbone carbonyl of Tyr 147.

The distance between the alpha-carbon (Cα) and the nitrogen atom in aliphatic ring of compound **14** with the nitrogen atom in aliphatic ring of epibatidine was calculated. The results suggested that the Cα-N distance (1.08 Å) was shorter than N–N distance (2.24 Å). It should be noted that, if this overlapped conformation is true for epibatidine and compound **14** in complex with AChBP, a change of 4-piperidinyl substitution to 3-piperidinyl substitution might fit compound **14** to epibatidine better and might contribute to significantly increased AChBP binding affinities. Thus, compound **15** with the expected 3-piperidinyl substitution was designed and synthesized (Scheme 3) during the 2nd round of optimization. Follow-up bio-assays suggested that compound **15** was a very potent AChBP ligand and was two orders of magnitude more potent than compound **14** (Table 1).

To explain the dramatically increased affinity of compound **15**, molecular docking was utilized. Since compound **15** had a chiral center, the binding modes of **(S)-15** and **(R)-15** were predicted separately. As shown in Figure 4, the protonated nitrogen atom of **(S)-15** shared two hydrogen bonds with Tyr 93 and Trp 147 and two cation-π interactions with Trp 147 and Tyr 188. At the same time, the protonated nitrogen atom of **(R)-15** only had one hydrogen-bond with Trp 147, but it also shared three cation-π interactions, two with Trp 148 and one with Tyr 195. The two aromatic rings of each enantiomer entered the same hydrophobic pockets as compound **14**. As the protonated nitrogen of epibatidine also shared a hydrogen-bond with Trp 147, it is possible that Trp 147 was a key residue for ligand-receptor interactions.

Enhancing interactions with Trp 147 might drastically increase the affinity of the compounds. Furthermore, as the aromatic rings entered the same pocket, changing the position of the protonated nitrogen atom altered the distance and the

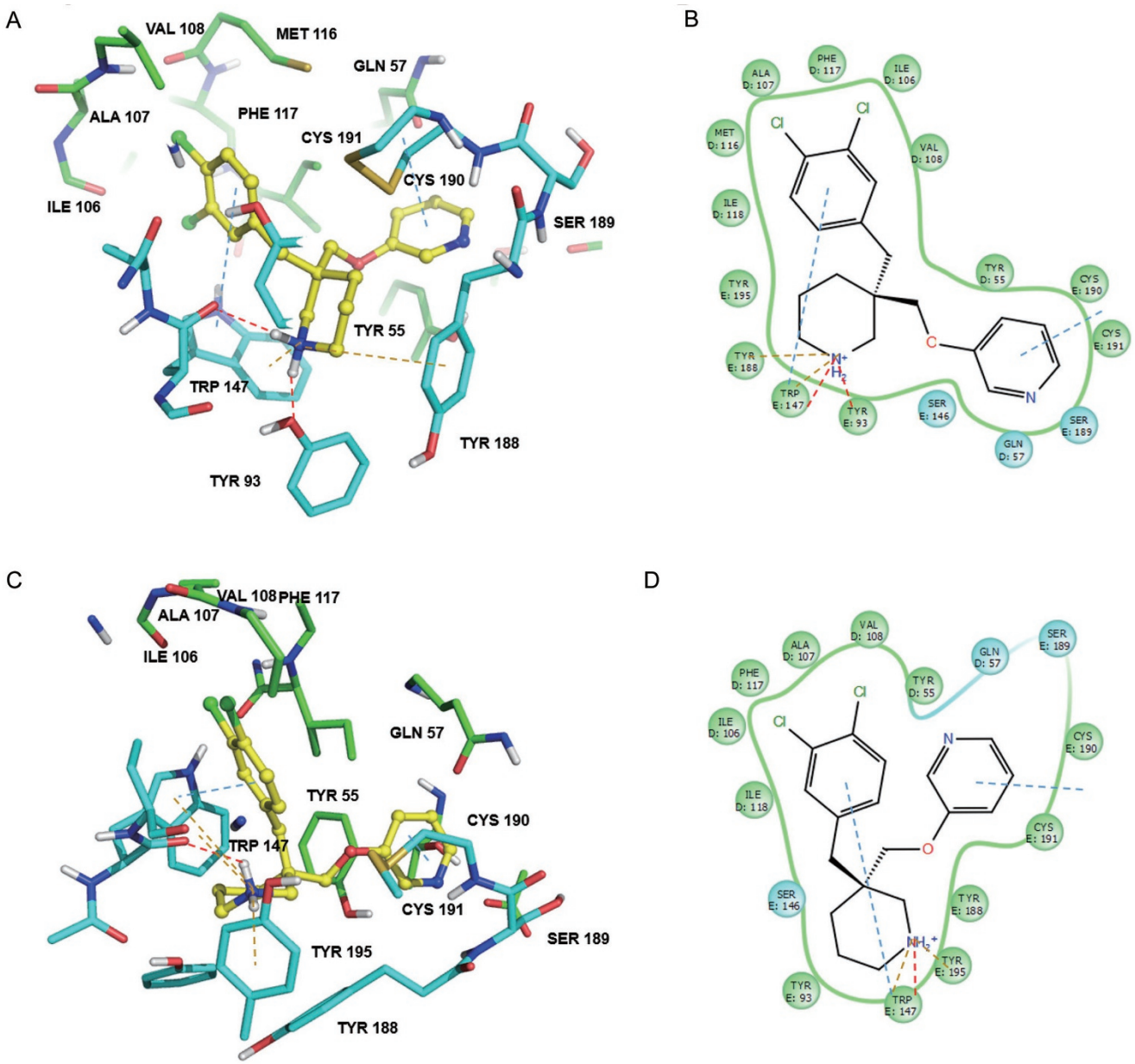

Figure 4. A putative binding mode of compound **(S)-15** and **(R)-15** in complex with Ls-AChBP. The hydrogen-bond (red dash), the cation-π interactions (brown dash) and the π–π interactions (blue dash) were shown. (A) The 3D view of the putative binding mode of compound **(S)-15** (colored by yellow). The principal side chain (colored by blue) and the complementary side (colored by green) were shown. (B) The 2D view of the putative binding mode of compound **(S)-15**. (C) The 3D view of the putative binding mode of compound **(R)-15** (colored by yellow). The principal side chain (colored by blue) and the complementary side (colored by green) were shown. (D) The 2D view of the putative binding mode of compound **(R)-15**.

orientation between the protonation center and the aromatic rings. Thus, changing the position of the protonated nitrogen atom may also improve the affinity of this compound.

In conclusion, pyridine-based compound **1** was identified from our in-house CNS-biased compound library by manual *in vitro* screening. With introduction of the privileged pyridine, compound **2** (21.5% inhibition at 100 nmol/L) was selected as the prototype compound for further optimization. Within the 1st of optimization, compound **14** displayed the highest binding affinity (K_i=105.6 nmol/L). Using the molecular docking results of compound **14** with Ls-AChBP, a 2nd of optimization was implemented with a structure-based strategy, which led to the discovery of the highly affinitive compound **15** (K_i=2.8 nmol/L) as a potent, novel, piperidine-based acetylcholine-binding protein ligand. The binding mode of compound **15** was then predicted to explain the drastic increase in binding affinity.

Acknowledgements

This work was supported by the Science and Technology Commission of Shanghai Municipality (No 15431900100) and the National Natural Science Foundation of China (No 81473076).

Author contribution

Li-ming SHAO, Lu ZHOU, and Wei LI conceived the research; Jian SHEN screened the in-house library based the biological assay which was set up by Lu ZHOU; Jian SHEN and Xi-cheng YANG designed and synthesized the target compounds, as well as biological assays under the supervision of Li-ming SHAO and Wei LI; Ming-cheng YU, Xun-jie ZHANG, Guan-xin PAN, Yu-rong YAN, and Si-chen WANG participated in synthetic works and biological assays; Xi-cheng YANG completed the works of molecular modeling; Yong-hui WANG, Qiong XIE, Lin-qian YU, Li XIAO, Hui-jiao SUN, and Hao CHEN were involved in data analysis and interpretation; Jian Shen and Xi-cheng Yang drafted the manuscript, which was revised and refined by Wei LI, Lu ZHOU, and Li-ming SHAO. All authors approved the final edition of manuscript.

Supplementary information

The supplementary information is available on the Acta Pharmacologica Sinica's website.

References

1 Ashford JW. Treatment of Alzheimer's disease: the legacy of the cholinergic hypothesis, neuroplasticity, and future directions. J Alzheimers Dis 2015; 47: 149–56.
2 Bensaid M, Michel PP, Clark SD, Hirsch EC, Francois C. Role of pedunculopontine cholinergic neurons in the vulnerability of nigral dopaminergic neurons in Parkinson's disease. Exp Neurol 2016; 275: 209–19.
3 Müller ML, Bohnen NI. Cholinergic dysfunction in Parkinson's disease. Curr Neurol Neurosci Rep 2013; 13: 377.
4 Perez XA. Preclinical evidence for a role of the nicotinic cholinergic system in Parkinson's disease. Neuropsychol Rev 2015; 25: 371–83.
5 Yarnall AJ, Del Din S, David R, Galna B, Baker MR, Burn DJ, *et al.* Cholinergic deficits contribute to impaired postural control in early Parkinson's disease. Movement Disord 2014; 29: S332–3.
6 Gibbons A, Dean B. The cholinergic system: an emerging drug target for schizophrenia. Curr Pharm Des 2016; 22: 2124–33.
7 Sarter M, Lustig C, Taylor SF. Cholinergic contributions to the cognitive symptoms of schizophrenia and the viability of cholinergic treatments. Neuropharmacology 2012; 62: 1544–53.
8 Scarr E, Dean B. Role of the cholinergic system in the pathology and treatment of schizophrenia. Expert Rev Neurother 2009; 9: 73–86.
9 Han Z, Li L, Wang L, Degos V, Maze M, Su H. Alpha-7 nicotinic acetylcholine receptor agonist treatment reduces neuroinflammation, oxidative stress, and brain injury in mice with ischemic stroke and bone fracture. J Neurochem 2014; 131: 498–508.
10 Skok M, Lykhmus O. The role of alpha 7 nicotinic acetylcholine receptors and alpha 7-specific antibodies in neuroinflammation related to Alzheimer disease. Curr Pharm Design 2016; 22: 2035–49.
11 Han Z, Shen F, He Y, Degos V, Camus M, Maze M, *et al.* Activation of alpha-7 nicotinic acetylcholine receptor reduces ischemic stroke injury through reduction of pro-inflammatory macrophages and oxidative stress. PLoS One 2014; 9: e105711.
12 Loram LC, Taylor FR, Strand KA, Maier SF, Speake JD, Jordan KG, *et al.* Systemic administration of an alpha-7 nicotinic acetylcholine agonist reverses neuropathic pain in male Sprague Dawley rats. J Pain 2012; 13: 1162–71.
13 Nikiforuk A, Kos T, Holuj M, Potasiewicz A, Popik P. Positive allosteric modulators of alpha 7 nicotinic acetylcholine receptors reverse ketamine-induced schizophrenia-like deficits in rats. Neuropharmacology 2016; 101: 389–400.
14 Bencherif M, Stachowiak MK, Kucinski AJ, Lippiello PM. Alpha7 nicotinic cholinergic neuromodulation may reconcile multiple neurotransmitter hypotheses of schizophrenia. Med Hypotheses 2012; 78: 594–600.
15 Young JW, Geyer MA. Evaluating the role of the alpha-7 nicotinic acetylcholine receptor in the pathophysiology and treatment of schizophrenia. Biochem Pharmacol 2013; 86: 1122–32.
16 Koike K, Hashimoto K, Takai N, Shimizu E, Komatsu N, Watanabe H, *et al.* Tropisetron improves deficits in auditory P50 suppression in schizophrenia. Schizophr Res 2005; 76: 67–72.
17 Hashimoto K. Targeting of alpha 7 nicotinic acetylcholine receptors in the treatment of schizophrenia and the use of auditory sensory gating as a translational biomarker. Curr Pharm Design 2015; 21: 3797–806.
18 Freedman R, Olincy A, Buchanan RW, Harris JG, Gold JM, Johnson L, *et al.* Initial phase 2 trial of a nicotinic agonist in schizophrenia. Am J Psychiat 2008; 165: 1040–7.
19 Olincy A, Harris JG, Johnson LL, Pender V, Kongs S, Allensworth D, *et al.* Proof-of-concept trial of an alpha 7 nicotinic agonist in schizophrenia. Arch Gen Psychiat 2006; 63: 630–8.
20 Hosford D, Dvergsten C, Beaver J, Segreti AC, Toler S, Farr MG, *et al.* Phase 2 clinical trial of TC-5619, an alpha 7 nicotinic receptor agonist in the treatment of negative and cognitive symptoms in schizophrenia. Eur Neuropsychopharm 2014; 24: S531–2.
21 Lieberman JA, Dunbar G, Segreti AC, Girgis RR, Seoane F, Beaver JS, *et al.* A randomized exploratory trial of an alpha-7 nicotinic receptor agonist (TC-5619) for cognitive enhancement in schizophrenia. Neuropsychopharmacology 2013; 38: 968–75.
22 Mazurov AA, Kombo DC, Hauser TA, Miao L, Dull G, Genus JF, *et al.* Discovery of (2S,3R)-N-[2-(Pyridin-3-ylmethyl)-1-azabicyclo[2.2.2]oct-3-yl]benzo[b]furan-2-carboxamide (TC-5619), a selective alpha 7 nicotinic acetylcholine receptor agonist, for the treatment of cognitive disorders. J Med Chem 2012; 55: 9793–809.
23 Preskorn SH, Gawryl M, Dgetluck N, Palfreyman M, Bauer LO, Hilt DC. Normalizing effects of EVP-6124, an alpha-7 nicotinic partial agonist, on event-related potentials and cognition: a proof of concept, randomized trial in patients with schizophrenia. J Psychiatr Pract 2014; 20: 12–23.
24 Kuca K, Soukup O, Maresova P, Korabecny J, Nepovimova E, Klimova B, *et al.* Current approaches against Alzheimer's disease in clinical trials. J Brazil Chem Soc 2016; 27: 641–9.
25 Di Paolo T, Gregoire L, Feuerbach D, Elbast W, Weiss M, Gomez-Mancilla B. AQW051, a novel and selective nicotinic acetylcholine receptor alpha 7 partial agonist, reduces L-Dopa-induced dyskinesias and extends the duration of *L*-dopa effects in parkinsonian monkeys. Parkinsonism Relat Disord 2014; 20: 1119–23.
26 Wu ZS, Cheng H, Jiang Y, Melcher K, Xu HE. Ion channels gated by acetylcholine and serotonin: structures, biology, and drug discovery. Acta Pharmacol Sin 2015; 36: 895–907.
27 Spurny R, Debaveye S, Farinha A, Veys K, Vos AM, Gossas T, *et al.* Molecular blueprint of allosteric binding sites in a homologue of the agonist-binding domain of the alpha 7 nicotinic acetylcholine recep-

tor. Proc Natl Acad Sci U S A 2015; 112: E2543–52.
28 Sauguet L, Shahsavar A, Poitevin F, Huon C, Menny A, Nemecz A, *et al.* Crystal structures of a pentameric ligand-gated ion channel provide a mechanism for activation. Proc Natl Acad Sci U S A 2014; 111: 966–71.
29 Chiodo L, Malliavin TE, Maragliano L, Cottone G, Ciccotti G. A structural model of the human alpha 7 nicotinic receptor in an open conformation. PLoS One 2015; 10: e0133011.
30 Beck ME, Gutbrod O, Matthiesen S. Insight into the binding mode of agonists of the nicotinic acetylcholine receptor from calculated electron densities. Chemphyschem 2015; 16: 2760–7.
31 Hu ZJ, Bai L, Tizabi Y, Southerland W. Computational modeling study of human nicotinic acetylcholine receptor for developing new drugs in the treatment of alcoholism. Interdiscip Sci 2009; 1: 254–62.
32 Smit AB, Syed NI, Schaap D, van Minnen J, Klumperman J, Kits KS, *et al.* A glia-derived acetylcholine-binding protein that modulates synaptic transmission. Nature 2001; 411: 261–8.
33 Brejc K, van Dijk WJ, Klaassen RV, Schuurmans M, van der Oost J, Smit AB, *et al.* Crystal structure of an ACh-binding protein reveals the ligand-binding domain of nicotinic receptors. Nature 2001; 411: 269–76.
34 Stornaiuolo M, De Kloe GE, Rucktooa P, Fish A, van Elk R, Edink ES, *et al.* Assembly of a pi-pi stack of ligands in the binding site of an acetylcholine-binding protein. Nat Commun 2013; 4: 1875.
35 Rucktooa P, Smit AB, Sixma TK. Insight in nAChR subtype selectivity from AChBP crystal structures. Biochem Pharmacol 2009; 78: 777–87.
36 Hansen SB, Sulzenbacher G, Huxford T, Marchot P, Taylor P, Bourne Y. Structures of Aplysia AChBP complexes with nicotinic agonists and antagonists reveal distinctive binding interfaces and conformations. EMBO J 2005; 24: 3635–46.
37 Celie PH, van Rossum-Fikkert SE, van Dijk WJ, Brejc K, Smit AB, Sixma TK. Nicotine and carbamylcholine binding to nicotinic acetylcholine receptors as studied in AChBP crystal structures. Neuron 2004; 41: 907–14.
38 Yamauchi JG, Gomez K, Grimster N, Dufouil M, Nemecz A, Fotsing JR, *et al.* Synthesis of selective agonists for the alpha 7 nicotinic acetylcholine receptor with *in situ* click-chemistry on acetylcholine-binding protein templates. Mol Pharmacol 2012; 82: 687–99.
39 Smit AB, Ulens C. From structure and function analysis in AChBP to drug design. FEBS J 2013; 280: 184.
40 Edink E, Akdemir A, Jansen C, van Elk R, Zuiderveld O, de Kanter FJ, *et al.* Structure-based design, synthesis and structure-activity relationships of dibenzosuberyl- and benzoate-substituted tropines as ligands for acetylcholine-binding protein. Bioorg Med Chem Lett 2012; 22: 1448–54.
41 de Kloe GE, Retra K, Geitmann M, Kallblad P, Nahar T, van Elk R, *et al.* Surface plasmon resonance biosensor based fragment screening using acetylcholine binding protein identifies ligand efficiency hot spots (LE hot spots) by deconstruction of nicotinic acetylcholine receptor alpha 7 ligands. J Med Chem 2010; 53: 7192–201.
42 Gundisch D, Eibl C. Nicotinic acetylcholine receptor ligands, a patent review (2006-2011). Expert Opin Ther Pat 2011; 21: 1867–96.
43 Yenugonda VM, Xiao YX, Levin ED, Rezvani AH, Tran T, Al-Muhtasib N, *et al.* Design, synthesis and discovery of picomolar selective alpha 4 beta 2 nicotinic acetylcholine receptor ligands. J Med Chem 2013; 56: 8404–21.
44 Zhang HK, Yu LF, Eaton JB, Whiteaker P, Onajole OK, Hanania T, *et al.* Chemistry, pharmacology, and behavioral studies identify chiral cyclopropanes as selective alpha 4 beta 2-nicotinic acetylcholine receptor partial agonists exhibiting an antidepressant profile. Part II. J Med Chem 2013; 56: 5495–504.
45 Jensen AA, Frolund B, Liljefors T, Krogsgaard-Larsen P. Neuronal nicotinic acetylcholine receptors: structural revelations, target identifications, and therapeutic inspirations. J Med Chem 2005; 48: 4705–45.
46 Li SX, Huang S, Bren N, Noridomi K, Dellisanti CD, Sine SM, *et al.* Ligand-binding domain of an alpha7-nicotinic receptor chimera and its complex with agonist. Nat Neurosci 2011; 14: 1253–9.